ELSEVIER

Journal of Alloys and Compounds 436 (2007) 124–130

Journal of ALLOYS AND COMPOUNDS

www.elsevier.com/locate/jallcom

The mechanical properties and microstructure of Al_2O_3/aluminum alloy composites fabricated by squeeze casting

Shang-Nan Chou [a], Jow-Lay Huang [a,*], Ding-Fwu Lii [b], Horng-Hwa Lu [c]

[a] *Department of Material Science and Engineering, National Cheng-Kung University, Tainan 701, Taiwan, ROC*
[b] *Department of Electrical Engineering, Cheng Shiu Institute of Technology, Kaohsiung County, Taiwan 833, ROC*
[c] *Department of Mechanical Engineering, National Chin-Yi Institute of Technology, Taiping, Taichung 411, Taiwan, ROC*

Received 17 May 2006; received in revised form 7 July 2006; accepted 7 July 2006
Available online 23 August 2006

Abstract

Porous aluminum oxide (Al_2O_3) preforms were formed by sintering in air at 1200 °C for 2 h. A356, 6061, and 1050 aluminum alloys were infiltrated into the preforms in order to fabricate Al_2O_3/A356, Al_2O_3/6061, and Al_2O_3/1050 composites, respectively, with different volumes of aluminum alloy content by squeeze casting. The volume contents of aluminum alloy in the composites were 10–40 vol.%. For the corresponding composites, the hardness decreased dramatically from 610 to 213, 201, and 153 HV, the four-points bending strength of the composites increased from 397 to 443, 435.1, and 418.7 MPa, and the fracture toughness increased from 4.97 to 11.35, 11.15, and 10.98 MPa $m^{1/2}$ of Al_2O_3/A356, Al_2O_3/6061, and Al_2O_3/1050 composites, respectively. From SEM microstructural analysis, the porous ratio and the relative density of the composites were the most important factors to affect the mechanical properties and the three different toughening mechanisms, i.e. crack bridging, crack deflection, and crack branching in the composites.
© 2006 Published by Elsevier B.V.

Keywords: Squeeze casting; Infiltration; Hardness; Four-points bending strength; Toughness

1. Introduction

Aluminum oxide (Al_2O_3) is a hard refractory ceramic, which has been investigated for high temperature structural and substrate applications because of its good strength and low thermal expansion coefficient. Nevertheless, like other monolithic ceramics, Al_2O_3 is apt to suffer from low ductility and low fracture toughness. Therefore, metals (e.g. aluminum, cobalt, niobium) or alloys are added to ceramics to improve their toughness [1–5].

Recently, the demands for lightweight materials having a high strength and a high toughness have attracted a lot of attention in the development of ceramic–matrix composites (CMCs). CMCs represent a new class of materials, which are on their way to substitute conventional materials in many fields. In the last few years considerable advances have been made in the development of manufacturing processes for CMCs, which have led to higher damage tolerance and a reduction in weight [6]. The most important limitation of the fabrication of CMCs by the liquid-phase process is caused by the compatibility of the reinforcement and the matrix [7]. This problem is especially important in the case of aluminum matrix composites, because aluminum is usually covered with a thin oxide layer which blocks surface wetting. Several methods have been investigated to improve the compatibility at the interface [8–11]. Squeeze casting is one of the most favorable processes, since the contact time between the reinforcement and the aluminum melt is short [12,13].

In this study, porous Al_2O_3 preforms were formed by sintering in air at 1200 °C for 2 h. Three different aluminum alloys were chosen to be the reinforcement in composites. Molten aluminum alloys A356, 6061, and 1050 were infil-

* Corresponding author. Tel.: +886 6 2348188; fax: +886 6 2763586.
E-mail address: jlh888@mail.ncku.edu.tw (J.-L. Huang).

0925-8388/$ – see front matter © 2006 Published by Elsevier B.V.
doi:10.1016/j.jallcom.2006.07.062

Table 1
The chemical composition of the aluminum alloys

	Si	Mg	Fe	Cu	Zn	Mn	Cr	Ti	Al
A356	7.13	0.63	0.11	<0.1	0.07	–	–	–	Rest
6061	0.8	1.1	0.7	0.2	0.25	0.15	0.15	0.15	Rest
1050	0.25	0.05	0.4	0.05	0.05	0.05	–	0.03	Rest

trated into the preforms to make Al_2O_3/A356, Al_2O_3/6061, and Al_2O_3/1050 composites, respectively, by squeeze casting. The physical and mechanical properties of the composites were measured. The effects of the composition on the physical and mechanical properties were also investigated. In addition, the microstructure and fracture behavior of the composites were examined.

2. Experimental

2.1. Sample preparation

The reinforced phases to improve strength and toughness of the Al_2O_3 ceramic matrix in this study were aluminum alloy A356, 6061, and 1050 (pure aluminum). The compositions are shown in Table 1. The Al_2O_3 powders were extracted from a thermally reactive process (A16SG ALCOA, USA), with a particle size being about 0.3–0.5 μm. The structure of the Al_2O_3 powders was α-phase, with purity higher than 99.8%. The selection of three different Al alloy compositions is simple and clear. We wanted to choose three similar but different kinds of Al alloy, so cast treatable alloy A356, heat treatable alloy 6061, and pure aluminum 1050 were selected. Nevertheless, in this experiment, we did not consider the heat treated state with the Al_2O_3/6061 composite because it was investigated in another experiment.

The Al_2O_3 powders were first mixed homogeneously with 10, 20, 30, and 40 vol.% of paraffin wax at 80 °C. The mixture was then placed in a stainless steel die to exert 20 MPa of pressure to form the Al_2O_3 preforms. Then, the preforms were thermally debinded at 300 °C for 2 h to remove paraffin wax and sintered in air at 1200 °C for 2 h. Porous Al_2O_3 preforms with pore contents of 10, 20, 30, and 40 vol.% were then made. The molten aluminum alloys A356 (about 690 °C), 6061 (about 740 °C), and 1050 (about 750 °C), were infiltrated into the preform to form Al_2O_3/A356, Al_2O_3/6061, and Al_2O_3/1050 composites. The squeeze casting processes included four steps: (a) preheating the casting die to 600 °C, and preparing molten A356 alloy; (b) Al_2O_3 preform setting (preheated in furnace to 600 °C); (c) high mechanical pressure for infiltration; and (d) release of pressure and extraction of the ingot [14]. During the squeeze casting process, the downward velocity of the squeeze head was 0.8–5 cm/s with a pressure of 200 MPa, and the loading time at high pressure was 30 s.

The composites were then cut and polished to 1 μm. Because the apparent difference between ceramic and aluminum alloy phases, the composites were not etched for scanning electron microscopy (SEM). The density and mechanical properties of the composites were measured. The effects of the composition on the physical and mechanical properties were investigated. In addition, the microstructure and fracture behavior of the composite were examined.

2.2. Density and mechanical properties

The density was measured by the water displacement technique. The hardness was determined applying a Vickers (Akashi AVK C21) indenter and calculated as $H = P/2d^2$, where d is the half-diagonal indentation impression and P is the indentation load (196 N for 15 s). Flexural strength was measured by a four-points bending test on an Instron universal testing machine (series 8511, Instron Co., Canton, MA, USA). The outer and inner spans were 40 and 20 mm, respectively. The nominal dimensions of the testing bars were 3 mm × 4 mm × 45 mm. Fracture toughness was measured in the same testing fixture using a Single Edge Notched Beam (SENB) method [15,16]. The maximum test load and the moment of the four-points bending load were used to calculate the toughness of the composite according to the following equation:

$$K_{IC} = \frac{6Ma^{1/2}}{db^2}Y$$

with:

$$M = \left(\frac{P}{2}\right)\frac{(L_1 - L_2)}{2}$$

$$Y = 1.99 - 2.74\left(\frac{a}{b}\right) + 12.97\left(\frac{a}{b}\right)^2 - 23.17\left(\frac{a}{b}\right)^3 + 24.80\left(\frac{a}{b}\right)^4$$

where P is the maximum test load, M the moment of the four-points bending load, d and b the width and height of the bending samples bar, respectively, a the depth of the single edge notch, L_1 and L_2 the outer and inner spans, respectively, and Y is the (a/b) ratio equation. For the stable crack growth mode in the Single Edge Notched Beam four-points bending specimen, it was suggested that $a/b = 1/2$, $L_1 = 40$ mm, and $L_2 = 20$ mm.

2.3. Microstructure analysis

The phases of the as-received Al_2O_3/A356 composites were analyzed by an X-ray diffractometer (Rigaku D/Max-II BX) using Cu Kα radiation (30 kV, 20 mA) in the range of 20–80° at a speed of 4° min^{-1}. The polished specimens of the composite were observed and characterized using an optical microscope (OM) and an image analyzer (Optimas, vol. 1.0, imaging Fundamentals, Tacoma, WA). Each image was divided into nine discrete elements (pixels), and entered into a digital computer to calculate the volume fraction of Al_2O_3/A356 composite. Fracture surfaces and crack propagation behavior were scrutinized using an OM and scanning electron microscopy (SEM, Hitachi S-4200). Etching was not necessary for optical microstructural examination due to the adequate contrast between the bright aluminum alloy and the dark Al_2O_3.

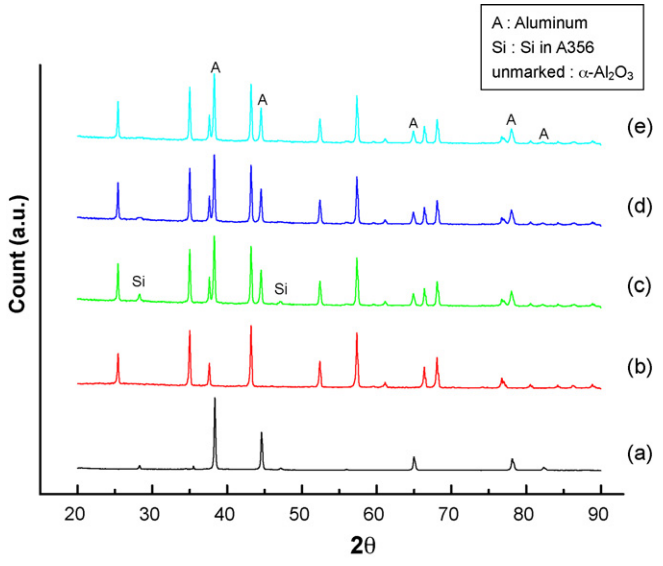

Fig. 1. X-ray diffraction patterns of (a) A356 aluminum alloy, (b) Al_2O_3 preform, (c) Al_2O_3/A356 composite, (d) Al_2O_3/6061 composite, and (e) Al_2O_3/1050 composite.

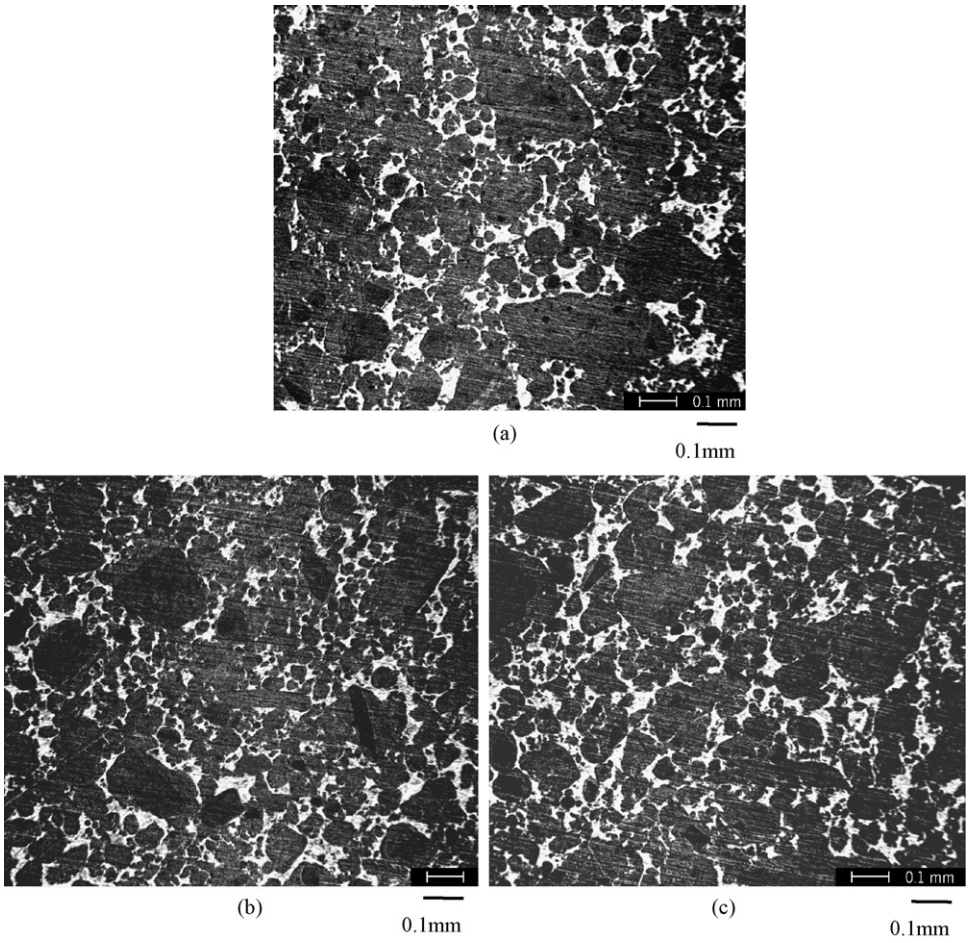

Fig. 2. Optical photographs showing the microstructure of include 40 vol.% aluminum alloy in Al_2O_3 composites. (a) A356 aluminum alloy, (b) 6061 aluminum alloy, and (c) 1050 aluminum alloy.

3. Results and discussions

3.1. Phase analysis

The X-ray diffraction patterns of (a) A356 aluminum alloy, (b) Al_2O_3 preform, (c) Al_2O_3/A356 composite, (d) Al_2O_3/6061 composite, and (e) Al_2O_3/1050 composite are shown in Fig. 1.

Fig. 1(c–e), respectively, shows the Al_2O_3/A356, Al_2O_3/6061, and Al_2O_3/1050 peaks. The composites consist only of α-Al_2O_3 ceramic and aluminum peak, and only the Al_2O_3/A356 composite has a diffraction patterns peak for its 7 wt.% silicon element content. Because of the stability of α-Al_2O_3 against molten aluminum alloys, no other reaction product in the compositions was found.

3.2. Compositional and microstructural analysis

All the composites were made from Al_2O_3 preforms at four aluminum alloy volume contents (10, 20, 30, and 40 vol.%). Typical optical photographs showing the microstructure of the Al_2O_3/aluminum alloy composites are shown in Fig. 2. These three pictures show that the Al_2O_3/aluminum alloy composites include 40 vol.% aluminum alloy, and the composites have a dense surface and a uniform distribution between the ceramic phase and alloy phase. Typical SEM polished surface micrographs showing the microstructure of the Al_2O_3/aluminum alloy composites are shown in Fig. 3. These three figures show that the Al_2O_3/aluminum alloy composites include 10 vol.% aluminum alloys and indicate that there is an almost dense surface in

Table 2
The physical and mechanical properties of the aluminum alloys

	Density (g/cm^3)	Melting point (°C)	Thermal expansion coefficient μm/(m K)	Hardness (HB)	Yield strength (MPa)
A356	2.71	560–580	21.5	75	235
6061	2.70	580–650	23.6	65	131
1050	2.705	660	23.6	32	103

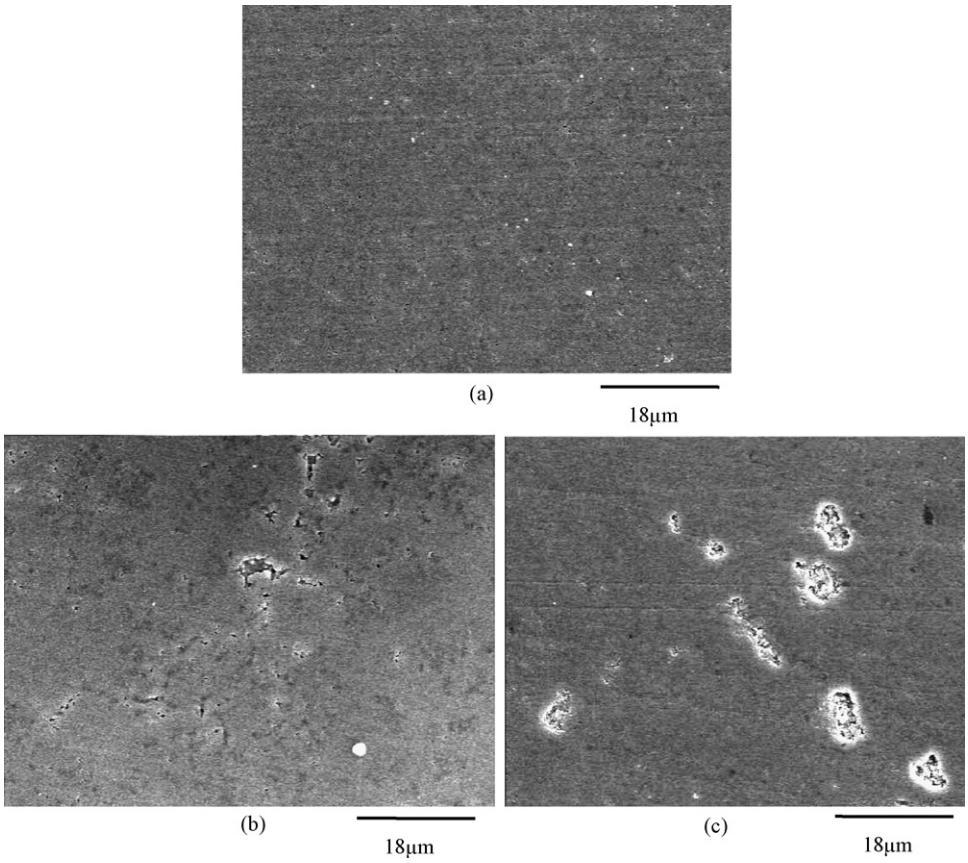

Fig. 3. SEM micro-photographs showing the microstructure of include 10 vol.% aluminum alloy in Al_2O_3 composites. (a) A356 aluminum alloy, (b) 6061 aluminum alloy, and (c) 1050 aluminum alloy.

Al_2O_3/A356 composites but there are several cavities and holes in the Al_2O_3/6061 and Al_2O_3/1050 composites. This is because the A356 alloy contains elementary silicon (Table 1) and has a wonderful fluid property and high mechanical pressure to exert upon the composites during squeeze casting process. Furthermore, these figures show that most of the voids are found in the middle of the ingot after the squeeze casting process, and these voids seriously influence the physical and mechanical properties of composites.

The Al_2O_3/aluminum alloy composites fabricated in this study contain 10–40 vol.% three kinds of aluminum alloy. The densities of these three aluminum alloys are about 2.70–2.71 g/cm^3 (Table 2), and the density of α-Al_2O_3 is 3.987 g/cm^3. The tendency of density change of the different Al_2O_3/aluminum alloy composites is shown in Fig. 4. The density (Fig. 4(a)) decreases with increasing aluminum alloy content from 10 to 40 vol.% almost linearly, and the relative density (Fig. 4(b)) of the composites increase with increasing aluminum alloy content from 10 to 40 vol.%. This is because the composites fabricated by squeeze casting with a high mechanical pressure of 200 MPa for 30 s. In the squeeze casting process, one can get more continue porous to infiltrate reinforcement inside preforms with increasing aluminum alloy content. One can get the relative density of composites content over 30 vol.% aluminum alloy were almost approached to 100%.

3.3. Mechanical properties

3.3.1. Hardness

The results of hardness measurements are shown in Fig. 5. The hardness decreased dramatically from 610 to 213, 201, and 153 HV with Al_2O_3/A356, Al_2O_3/6061, and Al_2O_3/1050 composites, respectively, by adding aluminum alloy from 10 to 40 vol.%. This is because aluminum alloy is a comparably soft material. The hardness of pure Al_2O_3 and pure aluminum alloys are shown in Table 2. The hardness of CMCs decreases with increasing aluminum alloy contents from 10 to 40 vol.%, but these three curves in Fig. 5 were basically similar. The hardness of all of the composites was approximate [17]. The imperceptible difference among them was the different hardness of aluminum alloys A356, 6061, and 1050. Therefore, the basic ceramic phase controls the hardness properties of the composites.

3.3.2. Bending strength and cross-section

Fig. 6 shows the four-points bending strengths relating to different aluminum alloy contents of the Al_2O_3/aluminum alloy composites. The four-points bending strength of the composites increased from 397 to 482.5 MPa, and from 397 to 463.3 MPa by increasing A356 and 6061 alloy contents from 0 to 10 vol.%, respectively, and then decreased from 482.5 to 443 MPa, and

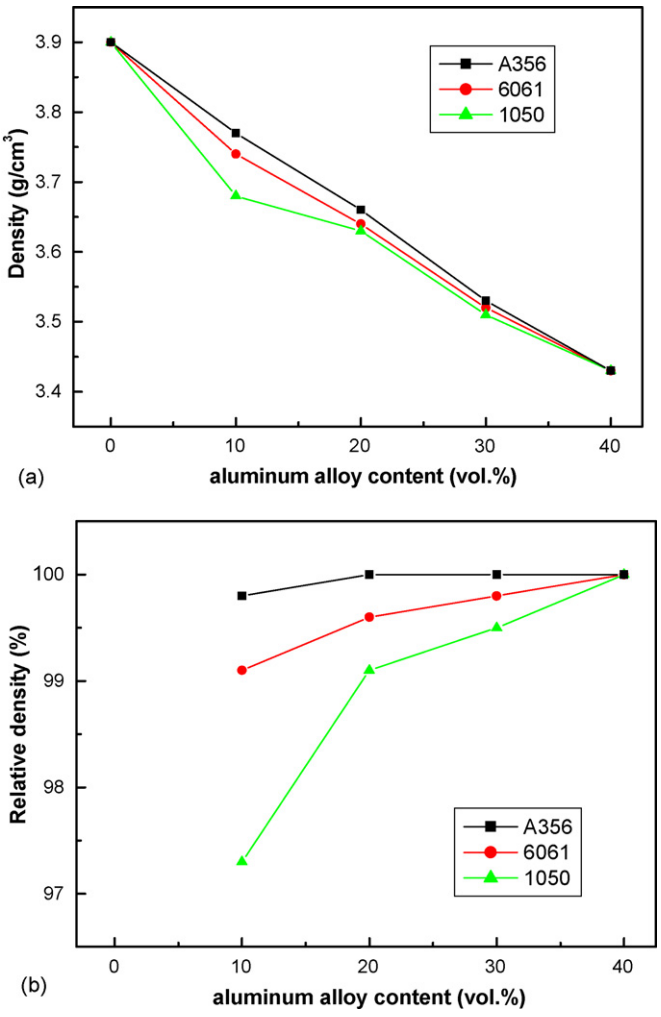

Fig. 4. The density (a) and relative density (b) vs. aluminum alloy content in the Al_2O_3/aluminum alloy composites.

from 463.3 to 435.1 MPa by further increasing A356 and 6061 alloy contents from 10 to 40 vol.%, respectively. This is because the relative density increased from 97.5 to about 100% (Fig. 4). Nevertheless, the strength decreases by increasing A356 content

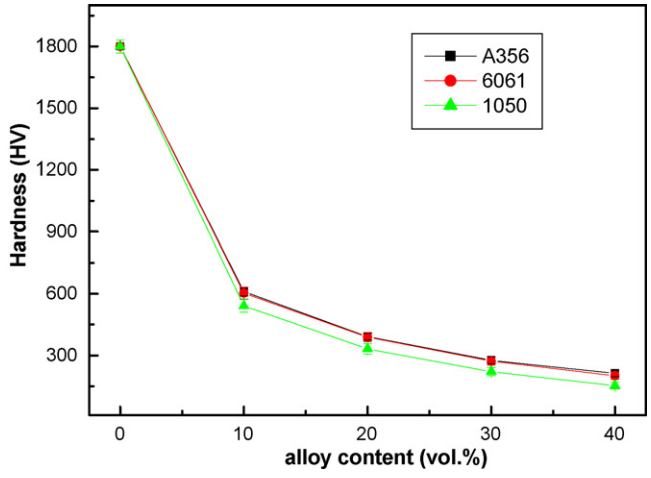

Fig. 5. Vickers hardness vs. aluminum alloy content in the composites.

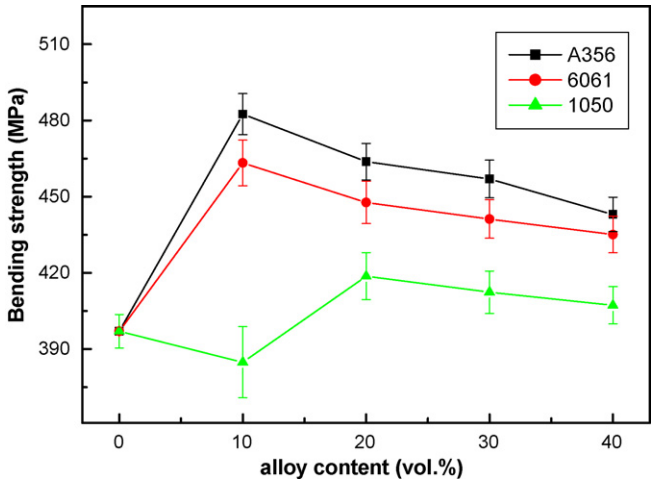

Fig. 6. Bending strength vs. aluminum alloy content in the composites.

from 10 to 40 vol.%, but the relative densities approach 100%; the strength decreases because the materials were infiltrated with a soft material aluminum alloy [17]. The same phenomenon was found in the bending strength of the Al_2O_3/1050 composite. It increased from 384.8 to 418.7 MPa by increasing the 1050 alloy contents from 10 to 20 vol.%. This is because the relative density approached 100%.

Fig. 7 shows the cross-section SEM micro-photographs of the Al_2O_3/aluminum alloy composites, including the 10 vol.% alloy, after four-points bending strength analyses of (a) A356 aluminum alloy, (b) 6061aluminum alloy, and (c) 1050 aluminum alloy in Al_2O_3/aluminum alloy composites. The figures show that the cross-section of the composites go from smooth and flat to undulated and ripply from Fig. 7(a–c). This is caused by discontinuous pores and voids inside the composite, and by the different mechanical properties of these three aluminum alloys. Due to there being more pores in Al_2O_3/A356, Al_2O_3/6061 than Al_2O_3/1050 composites, and the yield strength of A356 alloy is larger than 6061 and 1050 alloys (Table 2), one can detect the crack advance along these pores to appear increasingly undulated and ripply from Fig. 7(a–c). There are no pores in Fig. 7(a), because the Al_2O_3/A356 composite was very dense (relative density is equal to 99.8%). There are a few pores in Fig. 7(b) (arrow area), because the Al_2O_3/6061 composite was less dense (relative density is equal to 99.1%). There are more pores in Fig. 7(c) (arrow area), because the Al_2O_3/1050 composite was not dense (relative density is equal to 97.3%). The pores inside the composites were affecting the mechanical properties greatly. Therefore, the hardness of the Al_2O_3/A356 composite was larger than the Al_2O_3/6061 composite and the Al_2O_3/1050 composite with the same volume percentage aluminum alloy amount (10 vol.%).

3.3.3. *Fracture toughness and toughening mechanisms*

Fig. 8 shows the fracture toughness of the Al_2O_3/aluminum alloy composites with different contents of aluminum alloy. The fracture toughness increased from 4.97 to 11.35, 11.15,

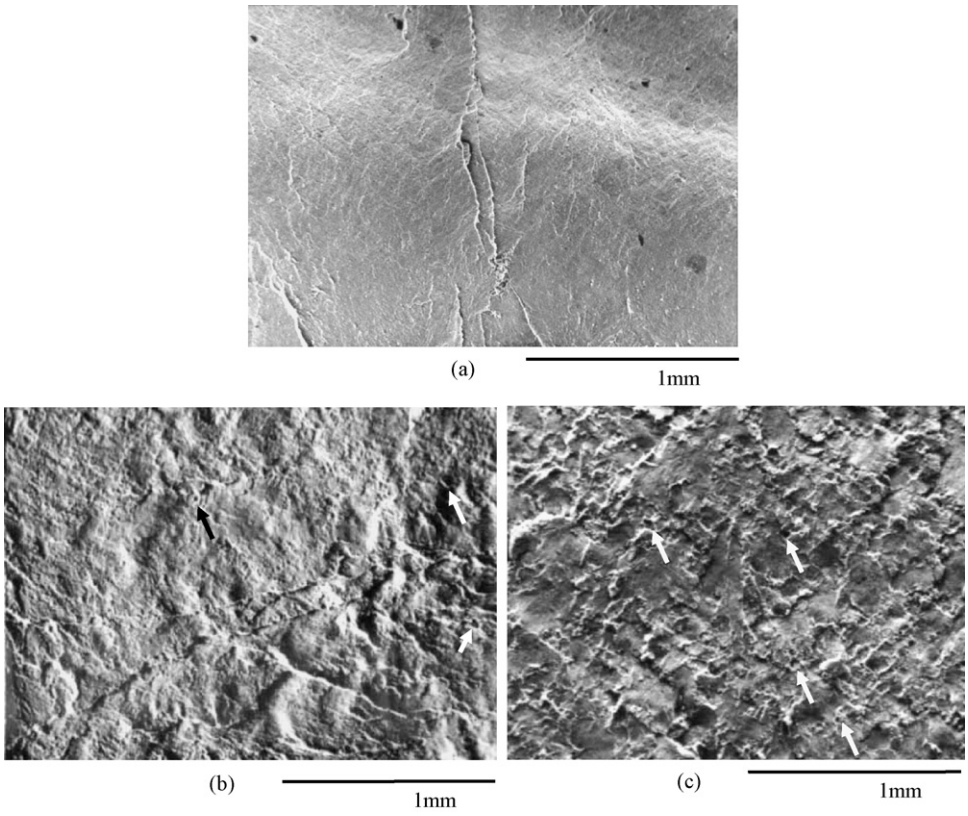

Fig. 7. The cross-section micro-photographs of Al_2O_3/aluminum alloy composites four-points bending properties (a) A356 aluminum alloy, (b) 6061 aluminum alloy, and (c) 1050 aluminum alloy in the Al_2O_3/aluminum alloy composites.

and 10.98 MPa $m^{1/2}$ by increasing A356, 6061, and 1050 alloy content, respectively, from 10 to 40 vol.%. The fracture toughness of all of these composites was higher than pure ceramic material, Al_2O_3. Because we infiltrated a high fracture toughness material, aluminum alloy A356, 6061, and 1050, the fracture toughness increased with increasing aluminum alloy content.

Crack bridging, crack deflection, and crack branching in the composites were observed in the SEM micrographs. These three conditions are the toughening mechanisms shown in Fig. 9. Fracture toughness means the capability to prevent and stop crack growth, and typically relies on these three toughening mechanisms [18–20], crack bridging, crack deflection, and crack branching, to scatter and remove the energy of crack growth, and then prevent and stop crack growth. Brittle ceramics can be toughened by incorporating ductile metallic inclusions into them [21]. If ductile metallic inclusions bridge a propagating crack, the ductile metallic inclusions can be stretched by the advancing crack until they are fractured or debonded. The stretching inclusions can absorb the fracture energy of a propagating crack, thus contributing to the toughness of brittle ceramics. The crack bridging (Fig. 9(a) arrow area) was the main item of three toughening mechanisms by soft materials in the composite. Erdogan et al. has suggested that the crack bridging toughening mechanism is effective as the bonding strength is in the intermediate range [22]. If the ductile metallic inclusions are strongly bonded to the ceramic matrix, the extent of inclusion will be limited, resulting in a limited toughness increase. Otherwise, if the bonding between the ceramic and metal is weak, the crack should propagate along the interfaces and deflect out of the plane that is normal to the applied tensile stress. Crack deflection (Fig. 9(b) arrow area) can scatter and dissipate the energy of cracks by increasing the crack length and making the crack turn. Crack branching (Fig. 9(c) arrow area) also increased the crack length of a major crack to several minor cracks.

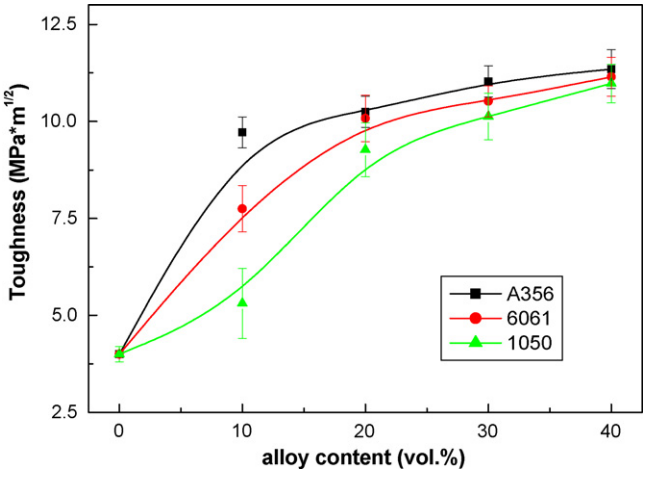

Fig. 8. Fracture toughness vs. aluminum alloy content in the composites.

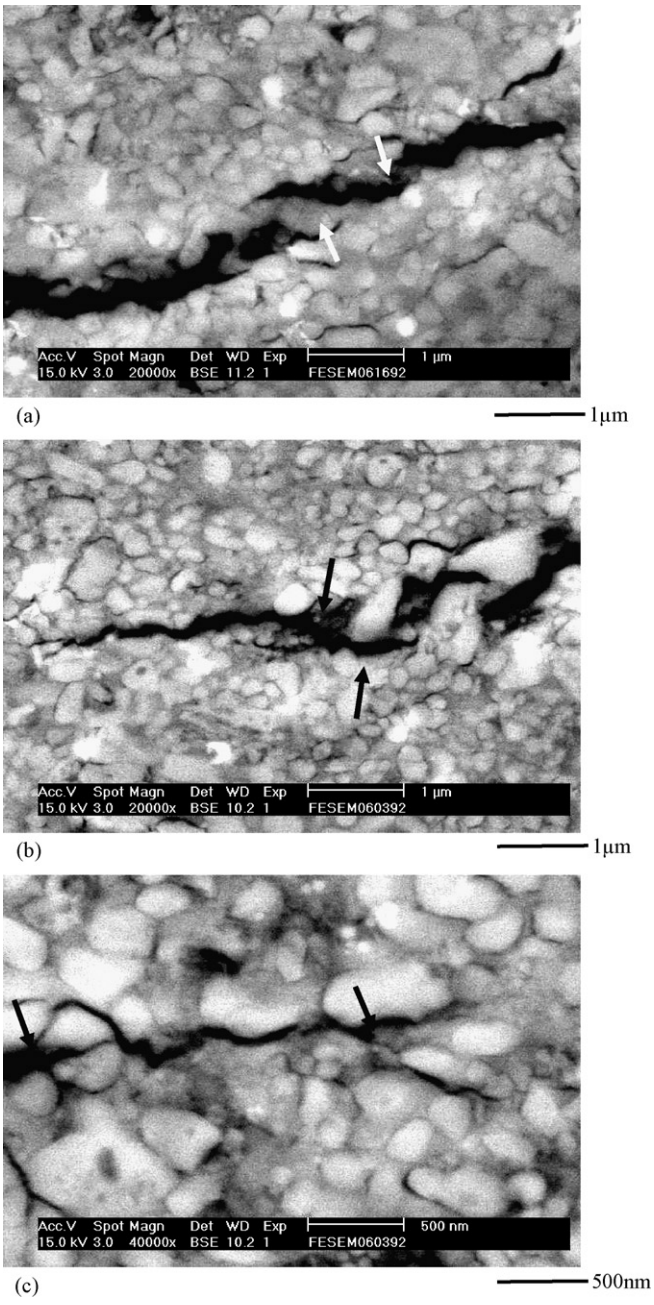

Fig. 9. Three toughening mechanisms (a) crack bridging, (b) crack deflection, and (c) crack branching in the Al_2O_3/A356 composites.

4. Conclusion

1. The density decreases linearly with increasing aluminum alloy content from 10 to 40 vol.%, and the relative densities of all composites were higher than 97.3%.
2. The hardness decreased dramatically from 610 to 213, 201, and 153 HV with Al_2O_3/A356, Al_2O_3/6061, and Al_2O_3/1050 composites, respectively, by increasing the aluminum alloy from 10 to 40 vol.%.
3. The four-points bending strength of the composites increased from 397 to 482.5 MPa, and from 397 to 463.3 MPa by increasing A356 and 6061 alloy content, respectively, from 0 to 10 vol.%, and then decreased from 482.5 to 443 MPa, and from 463.3 to 435.1 MPa by further increasing A356 and 6061 alloy content from 10 to 40 vol.%. The bending strength of Al_2O_3/1050 composite increased from 384.8 to 418.7 MPa by increasing the 1050 alloy content from 10 to 20 vol.%. This is because the relative density approached 100%.
4. The pores inside the composites affected the mechanical properties and the form of the cross-section greatly.
5. The fracture toughness increased from 4.97 to 11.35, 11.15, and 10.98 MPa $m^{1/2}$ by increasing A356, 6061, and 1050 alloy, respectively, content from 10 to 40 vol.%.
6. Three different toughening mechanisms, i.e. crack bridging, crack deflection, and crack branching in the composites were observed on SEM micrographs.

Acknowledgment

The authors would like to thank National Science Council of the Republic of China for its financial support under the Contract No. NSC-91-2622-E-006-061-CC3.

References

[1] C. Toy, W.D. Scott, J. Am. Ceram. Soc. 73 (1) (1990) 97–101.
[2] B.D. Flinn, M. Ruhle, A.G. Evans, Acta Metall. 37 (11) (1989) 3001–3006.
[3] D.C. Halverson, A.J. Pyzik, I.A. Aksay, W.E. Snowden, J. Am. Ceram. Soc. 72 (5) (1988) 775–780.
[4] L.S. Sigl, H.F. Fischmeister, Acta Metall. 36 (4) (1988) 887–897.
[5] L. Shaw, R. Abbaschian, J. Mater. Sci. 30 (1995) 849–854.
[6] A.G. Evans, R. Naslain (Eds.), Ceramic Transaction, vol. 58, The American Ceramic Society, 1995.
[7] A. Alonso, A. Pamies, J. Narciso, C. Garciacordovilla, E. Louis, Metall. Trans. 24A (6) (1993) 1423–1432.
[8] R. Smith, F.H. Fores, J. Metall. Mar. (1992) 85.
[9] L. Shy-Wen, D.D.L. Chung, J. Mater. Sci. 29 (1994) 3128–3150.
[10] P.K. Rohtagi, D. Nath, S.S. Singh, B.N. Keshavaram, J. Mater. Sci. 129 (1994) 5970.
[11] A.-B. Ma, H. Gan, T. Imura, Y. Nishida, J.Q. Jiang, M. Takagi, Mater. Trans. 38 (9) (1997) 812–816.
[12] C. Shuangjie, W. Renjie, Compos. Sci. Technol. 59 (1999) 157–162.
[13] A.M. Assar, M.A. Al-Nimir, J. Compos. Mater. 28 (1994) 1480.
[14] D.F. Lii, J.L. Huang, S.T. Chang, J. Eur. Ceram. Soci. 22 (2002) 253–261.
[15] G.K. Bansal, W.H. Duckworth, in: S.W. Freiman (Ed.), Fracture Mechanics Applied to Brittle Materials, STP 678, ASTM 38, 1973.
[16] R.F. Pabsi, in: R.C. Bradt, D.P.H. Hasselman, F.F. Lange (Eds.), Fracture Mechanics of Ceramics, Vol. 2, Microstructure, Materials, and Applications, Plenum Press, 1974, p. 555.
[17] S.N. Chou, J.L. Huang, D.F. Lii, H.H. Lu, J. Alloys Compd. 419 (2006) 98–102.
[18] A.G. Evans, in: J.A. Pask, A.G. Evans (Eds.), Ceramic Microstructures'86, Plenum Press, 1987, p. 775.
[19] R.W. Rice, Ceram. Eng. Sci. Proc. 6 (7–8) (1985) 589.
[20] R.W. Steinbrech, J. Eur. Ceram. Soc. 10 (1992) 131.
[21] W.H. Tuan, R.J. Brook, J. Eur. Ceram. Soc. 6 (1990) 31–37.
[22] F. Erdogan, P.F. Joseph, J. Am. Ceram. Soc. 72 (1989) 262.